Polymer Chemistry

PAPER

View Article Online
View Journal | View Issue

Cite this: *Polym. Chem.*, 2016, **7**, 402

An amphiphilic PEG-*b*-PFPE-*b*-PEG triblock copolymer: synthesis by CuAAC click chemistry and self-assembly in water†

Gérald Lopez,*[a] Marc Guerre,[a] Judith Schmidt,[b] Yeshayahu Talmon,[b] Vincent Ladmiral,[a] Jean-Pierre Habas[a] and Bruno Améduri*[a]

Received 7th October 2015,
Accepted 31st October 2015

DOI: 10.1039/c5py01621e

www.rsc.org/polymers

A new PEG_{2000}-*b*-$PFPE_{1200}$-*b*-PEG_{2000} amphiphilic triblock copolymer was synthesized by copper(I)-catalyzed alkyne–azide cycloaddition (CuAAC). The microstructure of this ABA triblock copolymer was unequivocally characterized by NMR spectroscopy. Diffusion-ordered spectroscopy (DOSY) NMR experiment revealed that ^{1}H resonances belonging to PEG and PFPE are aligned on the same horizontal line, thus implying that all these signals are due to the same macromolecule whose diffusion coefficient is lower than that of PEG and PFPE homopolymers. Thanks to its semi-fluorinated backbone bearing robust triazole rings, the PEG_{2000}-*b*-$PFPE_{1200}$-*b*-PEG_{2000} triblock copolymer exhibits good thermal stability with no significant weight loss until 275 °C under air. This triblock copolymer undergoes self-assembly into micelles (D = 10–20 nm) in aqueous solution as confirmed from cryogenic-temperature transmission electron microscopy, DOSY experiment in D_2O, and dynamic light scattering. The critical micelle concentration was determined by pyrene fluorescence assay, and was found to be 0.1 mg mL^{-1}.

Introduction

Amphiphilic block copolymers have attracted significant attention due to their ability to self-assemble into micelles, nanospheres, or vesicles.[1–4] These nanostructures have found applications in various fields such as controlled drug delivery, nano-reactors, or biomimetics.[5,6] Amphiphilic block copolymers are also used as dispersants, emulsifiers, wetting agents, flocculants, and demulsifiers in many industrial and pharmaceutical preparations.[1,7] Micelles have a hydrophobic compact inner core and a hydrophilic swollen outer shell in aqueous medium. In contrast to micelles formed from low molecular weight surfactants, block copolymer based micelles usually exhibit a better structural stability and allow easy control of the particle size.[8–10]

Poly(ethylene oxide) (PEO), also referred to as poly(ethylene glycol) (PEG), is often employed as the hydrophilic segment due to its biocompatibility, safety to handle, non-immunogenic, and non-antigenic properties.[11] The acronym PEO is generally used in reference to polymers with a molecular weight higher than 10 000 g mol^{-1}, whereas PEG is usually employed for lower molecular weight polymers.[11]

Interestingly, DeSimone *et al.*[12] have reported the surprising miscibility between low molecular weight PEG (M_n < 750 g mol^{-1}) and perfluoropolyethers (PFPEs). PFPEs belong to a unique class of chemically resistant, non-crystalline, and non-flammable fluoropolymers that exhibit low toxicity and very low glass transition temperatures (due to the higher flexibility of their backbone provided by the C–O–C ether bonds).[13]

PFPE-*b*-PEG-*b*-PFPE triblock copolymers are known to act as non-ionic fluorosurfactants that stabilize aqueous droplets in fluorocarbon oils,[14–16] while maintaining compatibility with biological systems.[17] Amphiphilic networks based on PEG and PFPE have also been prepared for fouling-release coatings applications.[18–20] Lodge *et al.*[21] have investigated the morphology of PEO-based triblock copolymer hydrogels using a combination of low-temperature scanning electron microscopy and contrast matched small-angle neutron scattering experiments. PFPE-*b*-PEO-*b*-PFPE triblock copolymers formed networks by aggregation of the end-blocks, but the PFPE blocks tended to adopt disk-like or even sheet-like structures.[21]

PFPEs under the Fomblin® Z trade name are used as reactive intermediates for polymer synthesis, thanks to their telechelic structure. For instance, α,ω-dihydroxy PFPEs (Fomblin® Z-DOL) have been employed for the synthesis of materials such as fluorinated polyurethanes,[22] epoxy or polyester

[a]*Institut Charles Gerhardt Montpellier UMR5253 CNRS-UM-ENSCM – Equipe Ingénierie et Architectures Macromoléculaires, Montpellier, France. E-mail: Gerald.Lopez@enscm.fr, Bruno.Ameduri@enscm.fr*
[b]*Department of Chemical Engineering, Technion-Israel Institute of Technology, Haifa 3200003, Israel*

†Electronic supplementary information (ESI) available: Full NMR and FTIR spectra. See DOI: 10.1039/c5py01621e

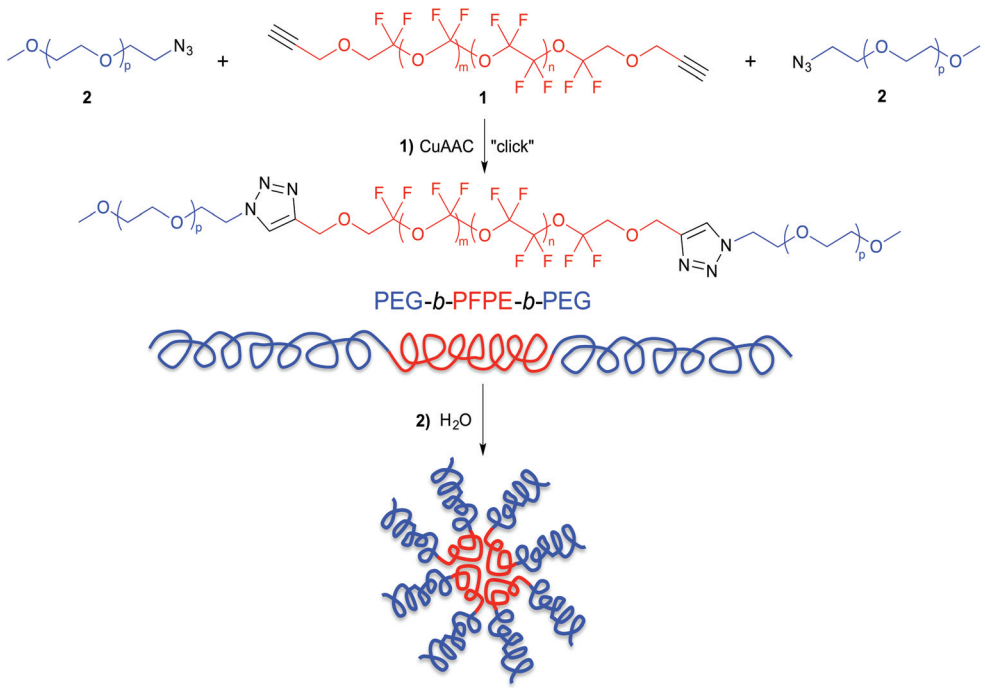

Scheme 1 (1) Synthesis of an amphiphilic PEG-*b*-PFPE-*b*-PEG triblock copolymer by copper(I)-catalyzed alkyne–azide cycloaddition (CuAAC) between PFPE–diyne **1** and PEG–azide **2**. Reaction conditions: CuBr/PMDETA (0.1 eq./0.1 eq.), DMF, 24 h, rt. (2) Self-assembly in water into micelles.

resins,[23,24] photocured or "clicked" fluoroelastomers,[25–29] PLA-PFPE-PLA triblock copolymers,[30,31] and electrolytes for lithium batteries.[32,33]

Xu *et al.*[34] have prepared a series of PFPE/PEG ABA and BAB triblock copolymers *via* thiol–ene click chemistry. Spin coated polymer films were characterized in detail by scanning electron microscopy (SEM) and atomic force microscopy (AFM), showing wrinkled continuous surfaces. Remarkable antibacterial properties were also observed, indicating once again that PFPE/PEG copolymers present a great potential for antimicrobial coating applications.

The present work describes a novel synthetic route to PEG-*b*-PFPE-*b*-PEG triblock copolymer using the very efficient copper(I)-catalyzed alkyne–azide cycloaddition (CuAAC) between PFPE diyne **1** (prepared in one step from Fomblin® Z-DOL) and PEG–azide **2** (Scheme 1). This triblock copolymer was thoroughly characterized by ^{1}H and ^{19}F-NMR spectroscopy and thermal analyses. The self-assembly behaviour in water of this ABA-type block copolymer was also precisely examined using different techniques, such as diffusion-ordered spectroscopy (DOSY) NMR, cryogenic-temperature transmission electron microscopy (cryo-TEM), dynamic light scattering (DLS), and pyrene fluorescence assay.

Experimental section

Materials

All organic solvents used for the syntheses were of analytical grade. Poly(tetrafluoroethylene oxide-*co*-difluoromethylene oxide)-α,ω-diol (Fomblin® Z-DOL, M_n = 1200 g mol^{-1}) was purchased from Alfa Aesar. Poly(ethylene glycol)methyl ether (M_n = 2000 g mol^{-1}), propargyl bromide solution (80 wt% in toluene, HC≡CH–CH$_2$–Br), sodium azide (NaN_3), *p*-toluenesulfonyl chloride (TsCl), copper(I) bromide (CuBr), and *N*,*N*,*N*′,*N*″,*N*″-pentamethyldiethylenetriamine (PMDETA) were purchased from Sigma-Aldrich. Deuterated solvents (D_2O and CD_3OD) for NMR characterization were purchased from Euriso-Top (Grenoble, France) (purity > 99.8%).

Measurements

Nuclear magnetic resonance (NMR). The NMR spectra were recorded on a Bruker AC 400 instrument. Coupling constants and chemical shifts are given in hertz (Hz) and parts per million (ppm), respectively. The experimental conditions for recording ^{1}H [or ^{19}F] NMR spectra were as follows: angle 90° [or 30°], acquisition time 4.5 s [or 0.7 s], pulse delay 2 s [or 5 s], number of scans 8 [or 16], and a pulse width of 5 μs for ^{19}F NMR. Diffusion-ordered NMR spectroscopy (DOSY) experiments were performed on a Bruker Avance III at 20 °C in 2.5 mm microtubes operating at 600 MHz with D_2O or CD_3OD as solvents.

Differential scanning calorimetry (DSC). DSC measurements were performed on 10–15 mg samples on a Netzsch DSC 200 F3 instrument. Two scans were recorded at a heating/cooling rate of 10 °C min^{-1} from −150 to 200 °C under an inert atmosphere (N_2) using aluminium standard crucibles with pierced aluminum lids. The glass transition temperatures (T_g) were reported at the inflection point of the heat capacity

jump of the second heating run. Melting transitions (T_m) were determined at the onset of the enthalpy peaks.

Thermogravimetric analysis (TGA). TGA analyses were carried out on 10–15 mg samples on a TGA Q50 apparatus from TA Instruments from 20 °C to 580 °C, in platinum pans, at a heating rate of 10 °C min^{-1}, under air.

Fourier transform infrared spectroscopy (FTIR). FTIR analyses were performed in the ATR mode using a Perkin-Elmer Spectrum 1000, with an accuracy of ±2 cm^{-1}.

Dynamic light scattering (DLS). Light scattering measurements were recorded on a VASCO-3 particle size analyzer from Cordouan Technologies. 1 mL samples were introduced into the cell after filtration through 0.45 μm PTFE microfilters.

Fluorimetry. Fluorimetry measurements were performed using a RF-5301PC spectrofluorophotometer (Shimadzu).

Cryogenic-temperature transmission electron microscopy (Cryo-TEM). Vitrified specimens were prepared in a controlled environment vitrification system (CEVS)[35] at 25 °C and 100% relative humidity. A drop (~3 μL) of the sample was placed on a perforated carbon film-coated copper grid, blotted with filter paper, and plunged into liquid ethane at its freezing point. The vitrified specimens were transferred to a 626 Gatan cryo-holder and observed at 120 kV acceleration voltage in an FEI Tecnai T12 G^2 transmission electron microscope at about −175 °C in the low-dose imaging mode to minimize electron-beam radiation damage. Images were digitally recorded with a Gatan US1000 high-resolution CCD camera.

Experimental

PFPE–diyne 1[29]

Poly(tetrafluoroethylene oxide-*co*-difluoromethylene oxide)-α,ω-diol (Fomblin® Z-DOL, Alfa Aesar, M_n = 1200 g mol^{-1} (Fig. 1), 20.0 g, 16.7 mmol) was suspended in a mixture of CH_3CN (80 mL) and THF (80 mL) containing sodium hydroxide (3.20 g, 83.5 mmol). This solution was heated to 55 °C under nitrogen. Propargyl bromide (80 wt% solution in toluene, 10.0 mL, 83.5 mmol) was added to the reaction mixture. The reaction mixture was heated under vigorous stirring at 55 °C for 3 days. The solution was then cooled, filtered over a medium frit and the solvent was evaporated. The crude product was further dried under high vacuum (40 × 10^{-3} mbar) at 100 °C and then purified by filtering through a 0.22 μm polyethersulfone filter to yield 17.5 g (82%) of a clear brown viscous oil. The product was analyzed by ^{19}F and ^{1}H-NMR spectroscopy (Fig. 2 and 3, respectively), and by FTIR spectroscopy (Fig. S2, ESI†).

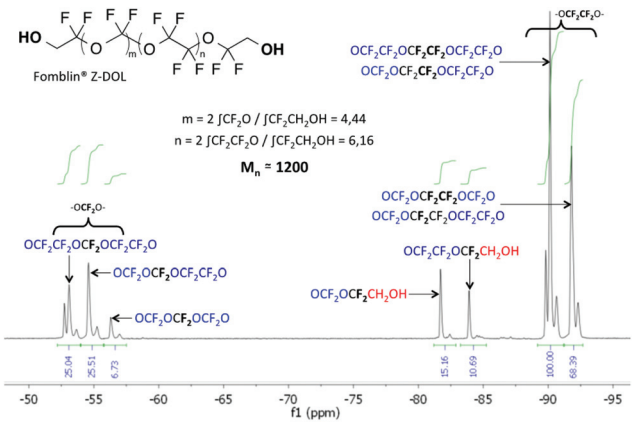

Fig. 1 ^{19}F NMR spectrum of poly(tetrafluoroethylene oxide-*co*-difluoromethylene oxide)-α,ω-diol (Fomblin® Z-DOL) recorded in CD_3OD.

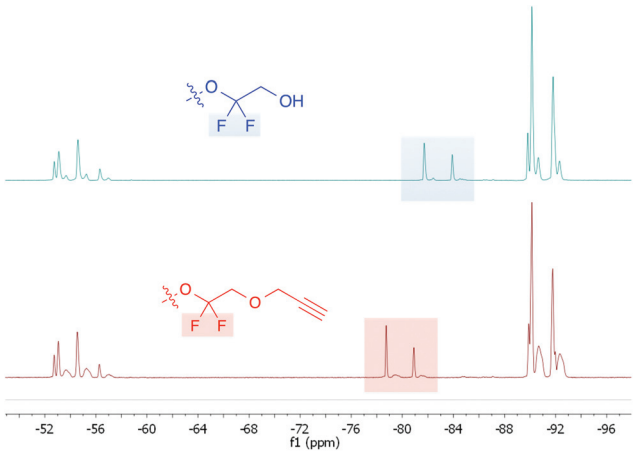

Fig. 2 ^{19}F NMR spectra overlay of poly(tetrafluoroethylene oxide-*co*-difluoromethylene oxide)-α,ω-diol (Fomblin® Z-DOL, top spectrum) and PFPE–diyne **1** (bottom spectrum) recorded in CD_3OD.

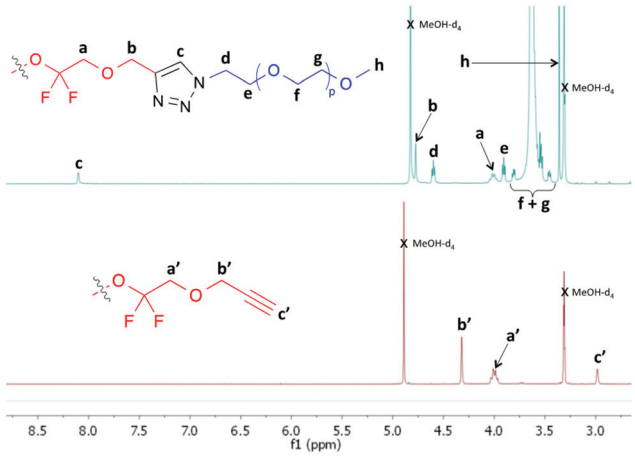

Fig. 3 ^{1}H NMR spectra overlay of the PEG_{2000}-*b*-$PFPE_{1200}$-*b*-PEG_{2000} triblock copolymer (top spectrum) and PFPE–diyne **1** (bottom spectrum) recorded in CD_3OD.

PEG–azide 2[36]

First, tosylated poly(ethylene glycol)methyl ether was synthesized according to the following procedure: poly(ethylene

glycol)methyl ether M_n = 2000 g mol^{-1} (5.00 g, 1 mmol) was dissolved in dry dichloromethane (25 mL) and triethylamine (1.50 mL, 10.8 mmol). To this solution, toluene-4-sulphonyl chloride (1.91 g, 10.0 mmol) was added at once. The reaction mixture was stirred at room temperature for 2 days under nitrogen. It was thereafter washed with water twice, and the organic phase was dried over $MgSO_4$. The solvent was removed and the remaining white solid was dissolved in a minimum amount of dichloromethane. To this solution, diethyl ether was added to precipitate the product. This purification step was repeated twice in order to obtain the pure product (70% yield).

Tosylated poly(ethylene glycol)methyl ether (2.50 g, 0.50 mmol) was then dissolved in 40 mL of dimethylformamide. To this solution, NaN_3 (325 mg, 5.00 mmol) was added at once, and the reaction mixture was stirred at room temperature for 2 days. Then, water and dichloromethane were added. The phases were separated, and the aqueous phase was extracted once more with dichloromethane. The organic phases were combined and washed three times with water, and the organic phase was dried over $MgSO_4$. The solvent was removed, and the residue was purified by precipitation in diethyl ether to yield a white solid (70% yield). The product was analyzed by ^{1}H-NMR spectroscopy (Fig. S3, ESI†).

PEG_{2000}-*b*-$PFPE_{1200}$-*b*-PEG_{2000} triblock copolymer

PFPE–diyne **1** (500 mg, 0.42 mmol, 1 eq.) and PEG–azide **2** (1.70 g, 0.83 mmol, 2 eq.) were suspended in DMF (20 mL). The mixture was degassed by bubbling nitrogen for 30 min. Then, copper(I) bromide (CuBr, 6.00 mg, 0.04 mmol, 0.1 eq.) and *N*,*N*,*N*′,*N*″,*N*″-pentamethyldiethylenetriamine (PMDETA, 7.00 mg, 0.08 mmol, 0.1 eq.) were added into the reaction mixture. After stirring for 24 h at room temperature, the reaction mixture was added dropwise to cold diethylether. After filtration, the slightly green powder was dried under vacuum until constant weight (95 wt%), then analyzed by FTIR spectroscopy (Fig. S6, ESI†) and by ^{19}F and ^{1}H-NMR spectroscopy (Fig. S5, ESI† and Fig. 3, respectively). The thermogravimetric (TGA) analysis revealed a decomposition temperature of 325 °C at 10% weight loss, under air (Fig. 4). Differential scanning calorimetry (DSC) showed a melting temperature (T_m) of 40 °C (Fig. S7, ESI†).

Fluorescence assay

First, a stock pyrene solution was prepared in acetone, and a known volume was transferred into a number of vials. The acetone was then evaporated before adding the block copolymer solutions to give a final pyrene concentration of 10^{-7} M. In each vial, block copolymer solutions (ranging from 0.002 to 1 mg mL^{-1}) were prepared by adding a known volume of a stock solution, and equilibrated for 24 h at room temperature. Fluorescence spectra of pyrene were recorded from 360 to 400 nm after excitation at 340 nm. The peak intensities at 372 and 383 nm were determined as I_1 and I_3, respectively (Fig. 9, inset). The ratios of the peak intensities I_3/I_1 of the emission spectra were recorded as a function of the block copolymer concentration (Fig. 9). The CMC value was determined by the intersection of the best-fit lines as shown in Fig. 9.

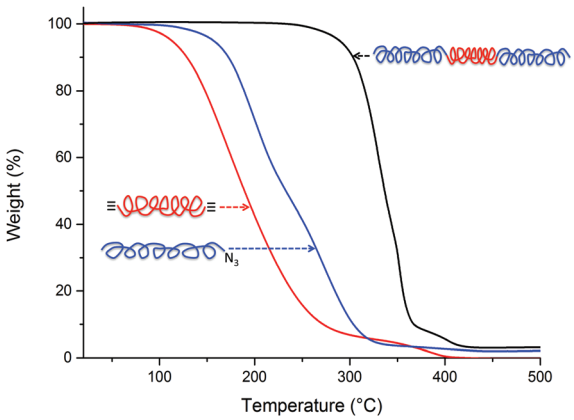

Fig. 4 TGA thermogram overlay of the PEG_{2000}-*b*-$PFPE_{1200}$-*b*-PEG_{2000} triblock copolymer (black curve), PEG–azide **2** (blue curve), and PFPE–diyne **1** (red curve), under air.

Results and discussion

Before going into details, it is worth mentioning that ^{19}F NMR spectroscopy is the method of choice to determine the structure of PFPEs, since it can reveal the number of OCF_2 and OCF_2CF_2 moieties, the end-groups, and thus the number-average molecular weight.[13,33] The ^{19}F NMR spectra of Fomblin® Z PFPEs display three distinct regions (Fig. 1): (i) from −50 to −60 ppm (OCF_2 groups), (ii) from −77 to −86 ppm (terminal CF_2 groups), and (iii) from −89 to −93 ppm (OCF_2CF_2 groups). The multiple peaks in each region arise from the different combinations of neighboring repeating units (see Fig. 1).

First, etherification at both ends of poly(tetrafluoroethylene oxide-*co*-difluoromethylene oxide)-α,ω-diol (Fomblin® Z-DOL) *via* SN_2 substitutions resulted in the formation of PFPE–diyne **1** in 82% yield.[29] A first glance at the ^{19}F NMR spectra overlay of Fomblin® Z-DOL and PFPE diyne **1** (Fig. 2) reveals that peaks from −81 to −84 ppm corresponding to the terminal CF_2CH_2OH groups of Fomblin® Z-DOL appear shifted downfield in the ^{19}F NMR spectrum of PFPE diyne **1**. A similar observation can be made on the corresponding ^{1}H NMR spectra overlay (Fig. S1, ESI†).

Further evidence of this substitution is the appearance of a narrow band at 3325 cm^{-1} (the CH stretch of terminal alkynes) in the FTIR spectrum of PFPE diyne **1**, while the free OH stretching absorption at 3400 cm^{-1} present in the FTIR spectrum of Fomblin® Z-DOL vanishes (Fig. S2, ESI†).

The hydrophilic part **2** of the triblock copolymer was obtained by using commercial hydroxyl end-functionalized PEG (M_n 2000 g mol^{-1}) that was chemically modified by tosylation then azidation, as previously described (the ^{1}H NMR spectrum of **2** is displayed in Fig. S3, ESI†).[36]

The two building blocks **1** and **2** were covalently coupled together *via* click chemistry[37] to afford the PEG_{2000}-*b*-$PFPE_{1200}$-*b*-PEG_{2000} triblock copolymer. To ensure the complete consumption of the reactive species, copper(I)-catalyzed alkyne–azide cycloaddition (CuAAC) was performed using two equivalents of **2** compared to **1**. Copper(I) bromide (0.1 mol eq.) and *N*,*N*,*N*′,*N*′,*N*″-pentamethyldiethylenetriamine (PMDETA, 0.1 mol eq.) were employed as the catalyst and the ligand, respectively.

Aliphatic amine ligands such as PMDETA are known to produce significant rate enhancements compared to pyridine-based ligands.[38]

After one day at room temperature, the PEG_{2000}-*b*-$PFPE_{1200}$-*b*-PEG_{2000} triblock copolymer was recovered by precipitation (>95 wt% yield). Nevertheless, it is worth mentioning that metal catalysts are known to form complexes with triazole rings, thus rendering the purification procedures non-trivial.[39]

The disappearance of terminal alkyne signals at δ = 3.05 ppm (see the ^{1}H NMR spectrum of **1** in Fig. S4, ESI†) and the appearance of triazole protons that resonate at δ = 8.10 ppm in the ^{1}H NMR spectrum of the PEG_{2000}-*b*-$PFPE_{1200}$-*b*-PEG_{2000} triblock copolymer (Fig. 3) are clear evidence of successful click reactions. In contrast, the ^{19}F NMR spectrum of the PEG_{2000}-*b*-$PFPE_{1200}$-*b*-PEG_{2000} triblock copolymer is almost similar to that of **1** (Fig. S5, ESI†).

The absence of bands at 3325 cm^{-1} (CH stretching of terminal alkynes) and 2100 cm^{-1} (azide stretching) in the FTIR spectra of the PEG_{2000}-*b*-$PFPE_{1200}$-*b*-PEG_{2000} triblock copolymer (Fig. S6, ESI†) provides another evidence of successful 1,3-dipolar cycloadditions, yet the absorptions at 1636 and 1457 cm^{-1} characteristic of triazole rings are too small to be observed. The FTIR spectrum of the PEG_{2000}-*b*-$PFPE_{1200}$-*b*-PEG_{2000} triblock copolymer also shows the bands from 1000 to 1250 cm^{-1} typically attributed to CF_2 groups and C–O–C moieties.[40]

The PEG_{2000}-*b*-$PFPE_{1200}$-*b*-PEG_{2000} triblock copolymer displays an improved thermal behavior over its precursors, as revealed by thermogravimetric analyses under air (Fig. 4). Indeed, thanks to its semi-fluorinated backbone bearing robust triazole rings, no significant weight loss was observed until 275 °C. The superior thermal stability of the triblock copolymer is most likely due to (i) its higher molecular weight, and (ii) the absence of azide and alkyne end-groups.

Indeed, the decomposition at lower temperatures of **1** and **2** under an oxidative atmosphere can be attributed to the rapid oxidation of azide and alkyne end-groups that leads to terminal radicals from which the chains unzip.[41]

The thermal transitions were studied by differential scanning calorimetry (DSC). For the PEG_{2000}-*b*-$PFPE_{1200}$-*b*-PEG_{2000} triblock copolymer, crystallization and melting processes are detected as exothermic and endothermic peaks at 28 and 57 °C, respectively (Fig. S7, ESI†). These values are in good agreement with those found for PEG–azide **2** (Fig. S8, ESI†). Nevertheless, the glass transition temperature of PFPE, generally observable at *ca.* −100 °C, is not displayed in the DSC thermogram of the PEG_{2000}-*b*-$PFPE_{1200}$-*b*-PEG_{2000} triblock copolymer since the difference in the heat capacity of this transition is too small compared to that of the melting temperature of PEG.

Diffusion-ordered spectroscopy (DOSY) NMR is increasingly employed for the characterization of block copolymers, since it is a fast and reliable technique to identify and account for the presence of residual homopolymers in solution.[42,43] Based on the Pulsed Gradient Spin Echo (PGSE) experiment,[44] DOSY-NMR leads to 2D correlation maps showing chemical shifts and diffusion coefficients on the horizontal and vertical axes, respectively. DOSY-NMR of the PEG_{2000}-*b*-$PFPE_{1200}$-*b*-PEG_{2000} triblock copolymer was achieved in CD_3OD (Fig. 5). The DOSY map shows an expanded view of the DOSY experiment with the related ^{1}H spectrum projected on top.

The ^{1}H NMR spectrum exhibits signals corresponding to the PFPE block (red arrows, Fig. 5) and PEG blocks (blue arrows, Fig. 5). As shown on the DOSY map, ^{1}H NMR signals belonging to PFPE and PEG correlate with the one and only diffusion coefficient (1.862×10^{-10} m^2 s^{-1}). To confirm that no residual PFPE–diyne and PEG–azide remain, CD_3OD solutions of **1** and **2** were analyzed by DOSY-NMR and were compared to the PEG_{2000}-*b*-$PFPE_{1200}$-*b*-PEG_{2000} triblock copolymer (Fig. 5, red inset for **1** and blue inset for **2**). The diffusion coefficients of **1** and **2** were found to be 6.310×10^{-10} m^2 s^{-1} and 2.138×10^{-10} m^2 s^{-1}, respectively.

Hence, no residual **1** or **2** was observed on the DOSY map of the triblock copolymer. DOSY-NMR, sometimes called "NMR chromatography", appears complementary to SEC chromatography, which was not possible in our case due to solubility issues.

To further analyze the ability of the PEG_{2000}-*b*-$PFPE_{1200}$-*b*-PEG_{2000} triblock copolymer to self-assemble, a 50 mg mL^{-1} aqueous solution was analyzed by dynamic light scattering (DLS). The results displayed in Fig. 6 show the formation of spheres of *ca.* 20 nm. A glance toward a higher diameter range

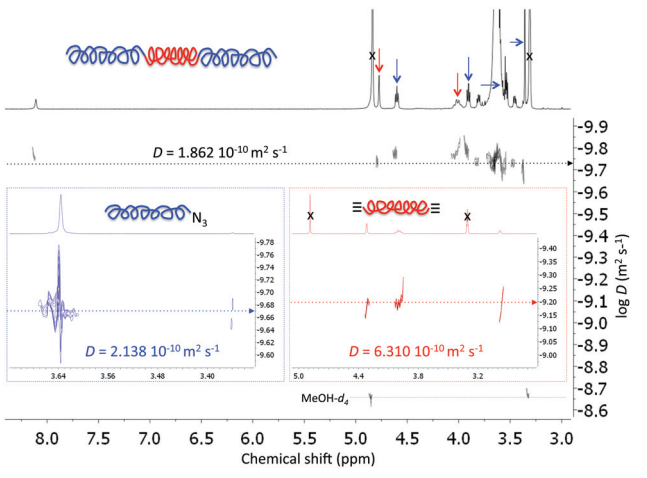

Fig. 5 ^{1}H DOSY-NMR spectra of the PEG_{2000}-*b*-$PFPE_{1200}$-*b*-PEG_{2000} triblock copolymer (main spectrum), PFPE–diyne **1** (red inset), and PEG–azide **2** (blue inset) recorded in CD_3OD. *D* = diffusion coefficient.

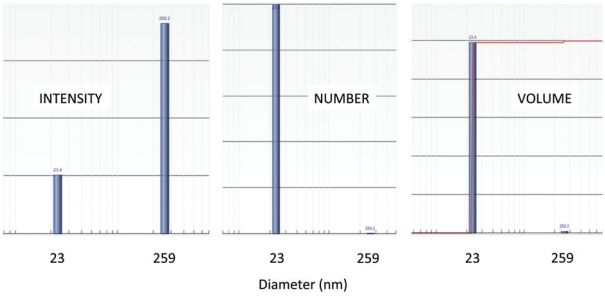

Fig. 6 DLS measurements for a 50 mg mL^{-1} aqueous solution of the PEG$_{2000}$-*b*-PFPE$_{1200}$-*b*-PEG$_{2000}$ triblock copolymer.

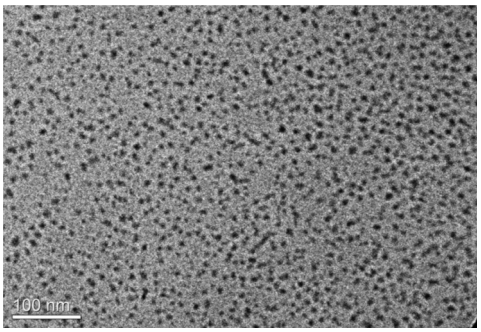

Fig. 8 Cryo-TEM image of the PEG$_{2000}$-*b*-PFPE$_{1200}$-*b*-PEG$_{2000}$ triblock copolymer in aqueous solution at a concentration of 50 mg mL^{-1}.

also indicates the presence of a negligible amount of bigger aggregates (*ca.* 260 nm). It is well established that the light intensity scattered by a 100 nm particle is equivalent to the light scattered by one million 10 nm-diameter particles and one trillion 1 nm-diameter particles of the same materials.[45]

Hence, the intensity of 259 nm-diameter particles is much higher than that of 23 nm-diameter particles.

DOSY-NMR has also been extensively used to measure the size of different materials, including lipid vesicles,[46] gold nanoparticles,[47] and photo-active amphiphilic polyoxazolines.[48] Therefore, assuming that all the species are spherical,[49] the size of the PEG$_{2000}$-*b*-PFPE$_{1200}$-*b*-PEG$_{2000}$ micelles was calculated using both the diffusion coefficient obtained from the DOSY-NMR experiment recorded in D_2O and the Stokes–Einstein equation (Fig. 7). The results show that the micelles have a radius of 10 nm (*ca.* 20 nm diameter). As expected, the diffusion coefficient is one order of magnitude smaller than that observed for the same polymer in solution (Fig. 5).

To check the morphology of the micelles, an aqueous solution of the PEG$_{2000}$-*b*-PFPE$_{1200}$-*b*-PEG$_{2000}$ triblock copolymer (50 mg mL^{-1}) was examined by cryogenic-temperature transmission electron microscopy (cryo-TEM).[50]

Fig. 8 and S9 (ESI†) show the corresponding image that clearly revealed the formation of nearly monodisperse spherical micelles of diameters in the range of 10–15 nm.

Since Kalyanasundaram and Thomas[51] proved that the characteristic dependence of the fluorescence vibrational fine structure of pyrene could be used to determine the critical micelle concentrations (CMC) of surfactant solutions, the so-called pyrene 1 : 3 ratio method has become one of the most popular procedures for the determination of this important parameter in micellar systems.[52,53] The plot of the pyrene 1 : 3 ratio as a function of the total surfactant concentration shows, around the CMC, a typical sigmoidal decrease. Below the CMC, the pyrene 1 : 3 ratio value corresponds to a polar environment. As the surfactant concentration increases, the pyrene 1 : 3 ratio decreases rapidly, indicating that the pyrene is sensing a more hydrophobic environment. Above the CMC, the pyrene 1 : 3 ratio reaches a roughly constant value because of the incorporation of the probe into the hydrophobic region of the micelles.

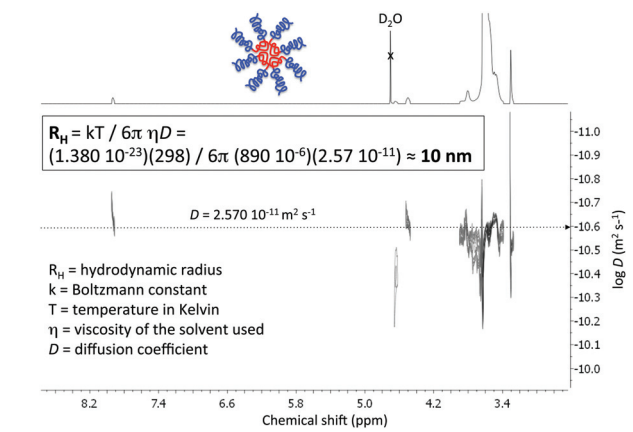

Fig. 7 ^{1}H DOSY-NMR spectrum of the PEG$_{2000}$-*b*-PFPE$_{1200}$-*b*-PEG$_{2000}$ triblock copolymer recorded in D_2O. Estimate of micelle radius size using the Stokes–Einstein equation.

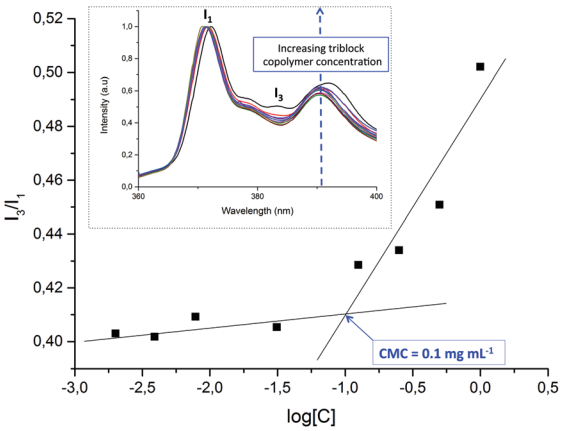

Fig. 9 Normalized emission spectra of pyrene in the presence of different PEG$_{2000}$-*b*-PFPE$_{1200}$-*b*-PEG$_{2000}$ triblock copolymer aqueous solutions. Inset represents the plot of fluorescence vibronic intensities ratio (I_3/I_1) as a function of the triblock copolymer concentration as measured from emission spectra (see Fig. S10, ESI†).

To assess the CMC of the PEG_{2000}-*b*-$PFPE_{1200}$-*b*-PEG_{2000} triblock copolymer in water, fluorimetry was carried out in emission with an excitation wavelength at 340 nm. Pyrene was used as the fluorescent probe with a concentration of 6×10^{-7} M. The intensity ratio (I_3/I_1) of pyrene emission spectra was plotted against the copolymer concentration (Fig. 9). The CMC was determined as the intersection of regression lines calculated from the two linear portions of the plot and was found to be 0.1 mg mL^{-1} (Fig. 9).

Conclusions

For the first time, a PEG_{2000}-based amphiphilic triblock copolymer containing a $PFPE_{1200}$ central core was synthesized by copper(I)-catalyzed alkyne–azide cycloaddition (CuAAC). Such an ABA triblock copolymer was thoroughly characterized by ^1H and ^{19}F-NMR spectroscopy. Diffusion-ordered spectroscopy (DOSY) NMR experiment accounted for the absence of residual homopolymers in solution. The PEG_{2000}-*b*-$PFPE_{1200}$-*b*-PEG_{2000} triblock copolymer displays a good thermal stability under an oxidative environment with no significant weight loss until 275 °C. The higher thermal stability of the triblock copolymer over its precursors was attributed to a combination of a higher molecular weight and the absence of azide and alkyne end-groups, which under oxidative conditions, afford terminal radicals that lead to chains unzipping. The PEG_{2000}-*b*-$PFPE_{1200}$-*b*-PEG_{2000} triblock copolymer undergoes self-assembly into micelles in aqueous solution as confirmed by three different analytical techniques, namely DLS, DOSY-NMR, and cryo-TEM, which all unambiguously validated the formation of 10–20 nm spherical nanoassemblies. Fluorimetry measurements were performed, and indicated a critical micelle concentration (CMC) of 0.1 mg mL^{-1}. In further development of this work, our group aims at evaluating this triblock copolymer as an electrolyte for Li-ion batteries.

Acknowledgements

Karine Parra from "Laboratoire de Mesures Physiques, Université de Montpellier" is gratefully acknowledged for recording DOSY-NMR spectra. The authors also thank Gerard Puts from the University of Pretoria for discussions about the thermal stability of the PEG_{2000}-*b*-$PFPE_{1200}$-*b*-PEG_{2000} triblock copolymer. The cryo-TEM work was performed at the Technion Laboratory for Electron Microscopy of Soft Matter, supported by the Technion Russell Berrie Nanotechnology Institute (RBNI).

Notes and references

1 *Amphiphilic Block Copolymers: Self-Assembly and Applications*, ed. P. Alexandridis and B. Lindman, Elsevier, Amsterdam, 2000.
2 T. Smart, H. Lomas, M. Massignani, M. V. Flores-Merino, L. R. Perez and G. Battaglia, *Nano Today*, 2008, **3**, 38–46.
3 A. Blanazs, S. P. Armes and A. J. Ryan, *Macromol. Rapid Commun.*, 2009, **30**, 267–277.
4 Y. Mai and A. Eisenberg, *Chem. Soc. Rev.*, 2012, **41**, 5969–5985.
5 R. Savic, L. B. Luo, A. Eisenberg and D. Maysinger, *Science*, 2003, **300**, 615–618.
6 *Block Copolymers in Nanoscience*, ed. M. Lazzari, G. Liu and S. Lecommandoux, Wiley-VCH, Weinheim, 2006.
7 P.-H. Ni, M.-Z. Zhang, L.-J. Zhuge and S.-K. Fu, *J. Polym. Sci., Part A: Polym. Chem.*, 2002, **40**, 3734–3742.
8 C. L. Zhao, M. A. Winnik, G. Riess and M. D. Croucher, *Langmuir*, 1990, **6**, 514–516.
9 M. Wilhelm, C. L. Zhao, Y. Wang, R. Xu and M. A. Winnik, *Macromolecules*, 1991, **24**, 1033–1040.
10 J. R. Quintana, M. Villacampa and I. A. Katime, *Macromolecules*, 1993, **26**, 606–611.
11 M. L. Adams, A. Lavasanifar and G. S. Kwon, *J. Pharm. Sci.*, 2003, **92**, 1343–1355.
12 Z. Hu, L. Chen, D. E. Betts, A. Pandya, M. A. Hillmyer and J. M. DeSimone, *J. Am. Chem. Soc.*, 2008, **130**, 14244–14252.
13 J. Scheirs, in *Modern Fluoropolymers*, ed. J. Scheirs, Wiley Interscience, New York, 1997, ch. 24, pp. 435–485.
14 C. Holtze, A. C. Rowat, J. J. Agresti, J. B. Hutchison, F. E. Angilè, C. H. J. Schmitz, S. Köster, H. Duan, K. J. Humphry, R. A. Scanga, J. S. Johnson, D. Pisignano and D. A. Weitz, *Lab Chip*, 2008, **8**, 1632–1639.
15 S. Köster, F. E. Angilè, H. Duan, J. J. Agresti, A. Wintner, C. Schmitz, A. C. Rowat, C. A. Merten, D. Pisignano, A. D. Griffiths and D. A. Weitz, *Lab Chip*, 2008, **8**, 1110–1115.
16 L. Mazutis and A. D. Griffiths, *Lab Chip*, 2012, **12**, 1800–1806.
17 I. Platzman, J.-W. Janiesch and J. P. Spatz, *J. Am. Chem. Soc.*, 2008, **130**, 3339–3342.
18 Y. Wang, L. M. Pitet, J. A. Finlay, L. H. Brewer, G. Cone, D. E. Betts, M. E. Callow, J. A. Callow, D. E. Wendt, M. A. Hillmyer and J. M. DeSimone, *Biofouling*, 2011, **27**, 1139–1150.
19 Y. Wang, D. E. Betts, J. A. Finlay, L. Brewer, M. E. Callow, J. A. Callow, D. E. Wendt and J. M. DeSimone, *Macromolecules*, 2011, **44**, 878–885.
20 Y. Wang, J. A. Finlay, D. E. Betts, T. J. Merkel, J. C. Luft, M. E. Callow, J. A. Callow and J. M. DeSimone, *Langmuir*, 2011, **27**, 10365–10369.
21 R. R. Taribagil, M. A. Hillmyer and T. P. Lodge, *Macromolecules*, 2010, **43**, 5396–5404.
22 C. Tonelli, T. Trombetta, M. Scicchitano and G. Castiglioni, *J. Appl. Polym. Sci.*, 1995, **57**, 1031–1042.
23 L. Mascia, F. Zitouni and C. Tonelli, *Polym. Eng. Sci.*, 1995, **35**, 1069–1076.
24 M. Toselli, F. Pilati, M. Fusari, C. Tonelli and C. Castiglioni, *J. Appl. Polym. Sci.*, 1994, **54**, 2101–2106.
25 X. Yao, S. S. Dunn, P. Kim, M. Duffy, J. Alvarenga and J. Aizenberg, *Angew. Chem., Int. Ed.*, 2014, **53**, 1–6.
26 A. Vitale, M. Quaglio, S. L. Marasso, A. Chiodoni, M. Cocuzza and R. Bongiovanni, *Langmuir*, 2013, **29**, 15711–15718.

27 C. De Marco, A. Gaidukeviciute, R. Kiyan, S. M. Eaton, M. Levi, R. Osellame, B. N. Chichkov and S. Turri, *Langmuir*, 2013, **29**, 426–431.
28 Z. Hu, J. A. Finlay, L. Chen, D. E. Betts, M. A. Hillmyer, M. E. Callow, J. A. Callow and J. M. DeSimone, *Macromolecules*, 2009, **42**, 6999–7007.
29 Y.-W. Yang, J. Hentschel, Y.-C. Chen, M. Lazari, H. Zeng, M. R. van Dam and Z. Guan, *J. Mater. Chem.*, 2012, **22**, 1100–1106.
30 D. Haynes, A. K. Naskar, A. Singh, C.-C. Yang, K. J. Burg, M. Drews, G. Harrison and D. W. Smith Jr., *Macromolecules*, 2007, **40**, 9354–9360.
31 A. Singh, A. K. Naskar, D. Haynes, M. J. Drewsa and D. W. Smith Jr., *Polym. Int.*, 2011, **60**, 507–516.
32 D. H. C. Wong, J. L. Thelen, Y. Fu, D. Devaux, A. A. Pandya, V. S. Battaglia, N. P. Balsara and J. M. DeSimone, *Proc. Natl. Acad. Sci. U. S. A.*, 2014, **111**, 3327–3331.
33 D. H. C. Wong, A. Vitale, D. Devaux, A. Taylor, A. A. Pandya, D. T. Hallinan, J. L. Thelen, S. J. Mecham, S. F. Lux, A. M. Lapides, P. R. Resnick, T. J. Meyer, R. M. Kostecki, N. P. Balsara and J. M. DeSimone, *Chem. Mater.*, 2015, **27**, 597–603.
34 J. Song, Q. Ye, W. T. Lee, X. Wang, T. He, K. W. Shah and J. Xu, *RSC Adv.*, 2015, **5**, 64170–64179.
35 Y. Talmon, in *Modern Characterization Methods of Surfactants Systems*, ed. B. P. Binks, Modern Dekker, New York, 1999, ch. 5, pp. 147–178.
36 Y. S. Ko, M. V. Circu, T. Geiger, S. Dünki, F. A. Nüesch and D. M. Opris, *RSC Adv.*, 2014, **4**, 35027–35034.
37 H. C. Kolb, M. G. Finn and K. B. Sharpless, *Angew. Chem., Int. Ed.*, 2001, **40**, 2004–2021.
38 P. L. Golas, N. V. Tsarevsky, B. S. Sumerlin and K. Matyjaszewski, *Macromolecules*, 2006, **39**, 6451–6457.
39 A. Qin, L. Tang, J. W. Y. Lam, C. K. W. Jim, Y. Yu, H. Zhao, J. Sun and B. Z. Tang, *Adv. Funct. Mater.*, 2009, **19**, 1891–1900.
40 J. Pacansky, M. Miller, W. Hatton, B. Liu and A. Scheiner, *J. Am. Chem. Soc.*, 1991, **113**, 329–343.
41 C. L. Beyler and M. M. Hirschler, in *SFPE Handbook of Fire Protection Engineering*, ed. P. J. DiNenno, NFPA, Quincy, 2001, ch. 7, pp. 1–110.
42 S. Viela, M. Mazarin, R. Giordanengo, T. N. T. Phan, L. Charles, S. Caldarelli and D. Bertin, *Anal. Chim. Acta*, 2009, **654**, 45–48.
43 Y. Bakkour, V. Darcos, S. Li and J. Coudane, *Polym. Chem.*, 2012, **3**, 2006–2010.
44 B. Antalek, *Concepts Magn. Reson.*, 2002, **14**, 225–258.
45 B. J. Berne and R. Pecora, *Dynamic light scattering with application to chemistry, biology and physics*, Courier Dover, New York, 1976.
46 D. P. Hinton and C. S. Johnson Jr., *J. Phys. Chem.*, 1993, **97**, 9064–9072.
47 G. Canzi, A. A. Mrse and C. P. Kubiak, *J. Phys. Chem. C*, 2001, **115**, 7972–7978.
48 L. Korchia, C. Bouilhac, V. Lapinte, C. Travelet, R. Borsali and J.-J. Robin, *Polym. Chem.*, 2015, **6**, 6029–6039.
49 C. S. Johnson, *Prog. Nucl. Magn. Reson. Spectrosc.*, 1999, **34**, 203–256.
50 Y. Talmon, *J. Mol. Liq.*, 2015, **210**(A), 2–8.
51 K. Kalyanasundaram and J. K. Thomas, *J. Am. Chem. Soc.*, 1977, **99**, 2039–2044.
52 J. Aguiar, P. Carpena, J. A. Molina-Bolívar and C. Carnero Ruiz, *J. Colloid Interface Sci.*, 2003, **258**, 116–122.
53 J. Muller, F. Marchandeau, B. Prelot, J. Zajac, J.-J. Robin and S. Monge, *Polym. Chem.*, 2015, **6**, 3063–3073.